Journal of Himalayan Earth Sciences 42 (2009) 1-24

Petrogenesis of Plio-Pleistocene volcanic rocks from the Chagai arc, Balochistan, Pakistan

Rehan H. Siddiqui[1], M. Asif Khan[2], M. Qasim Jan[3] and M. Ogasawara[4]
[1]Geoscience Advance Research Laboratories, Geological Survey of Pakistan, Shahzad Town, Islamabad, Pakistan
[2]National Centre of Excellence in Geology, University of Peshawar, Pakistan
[3]Quaid-i-Azam University, Islamabad, Pakistan
[4]Geological Survey of Japan, AIST, Tsukuba, Japan

Abstract

The Plio-Pleistocene volcanic rocks, which are designated as Koh-e-Sultan Volcanic Group, occur in an east-west trending subduction related magmatic belt known as Chagai arc in the western part of Pakistan. The volcanism in this arc was initiated during the Late Cretaceous due to an intra-oceanic convergence in the Ceno-Tethys, which intermittently continued up to the Quaternary period. The latest episode of volcanism in this arc was marked by an explosive activity represented by pumice deposits of 0.09 ± 0.01 Ma (K-Ar whole rock age of pumice). Petrological studies of lava flows show several varieties of andesites and dacites, which include hypersthene, hornblende, lamprobolite andesites and hornblende biotite dacite. The andesites are medium-K (0.18-1.28 wt.% K_2O) and have low Mg # (47-64), and higher FeO (total) MgO (1.01-1.77) ratios, suggesting fractionated nature of the parent magma. The primordial mantle-normalised trace element patterns of andesites exhibit marked negative Nb anomalies with spikes generally on K, Sr and Ba. These geochemical signatures strongly confirm their island arc affinity that is also supported by their LREE enriched chondrite-normalised REE patterns. Their Zr/Y (5.07-9.08), Zr/Nb (17.75-28.75), Ti/V (24.22-33.91), La/Yb (9.07-11.87), Ta/Yb (0.11-1.18) and Th/Yb (1.69-2.25) ratios are consistent with calc-alkaline rocks of continental margin-type island arcs. The Zr versus Zr/Y studies suggest that these volcanics are fractionated from 15% partially melted enriched mantle source. The andesitic rocks from Koh-e-Sultan are more enriched in LILE as compared with the analogous rocks in the surrounding satellite cones and plugs. The average Plio-Pleistocene andesite from the Chagai arc shows relatively more resemblance in LILE, HFSE and REE with its counterpart in Zagros arc and less with Japan and Sunda arcs; it greatly differs in these elements with its counterpart in the Andes arc.

Keywords: Plio-Pleistocene volcanics; Chagai arc; Andean-type calc-alkaline affinities

1. Introduction

Plio-Peistocene volcanics are found in an east west-tending mountain belt, known as Chagai arc, also known as Chagai magmatic belt or Chagai hills, locatedin the west of the Balochistan province of Pakistan. Many important metal deposits, including porphyry (Mo-Au-Ag), manto and vein type copper, stratiform and skarn type iron, volcanogenic gold-silver and sulphure, kuroko type lead-zinc-silver-copper are intimately associated with the magmatic rocks of this arc. In addition, a variety of granites and green onyx marble (travertine) is also mined from this arc.

The Chagai-Makran region of this province is a unique tectonic regime in the eastern Middle East. It is bounded by the Makran subduction zone in the south, which is one of the rare surviving subduction zones of Cretaceous age; others like the Indus suture zone in the Himalayas and Zagros subduction in Iran having been eliminated by major continental collisions. The Chaman transform fault in the east and Harirud fault in the west bound the Makran region (Fig. 1). Much of the southern Makran region represents one of the biggest accretionary prisms on earth, occupying the hanging wall of the Makran subduction zone. This accretionary prism occurs at the southern margin of the Afghan microcontinent. The accretionary prism extends for 450 km to the north whereby it abates against two mountain ranges, Chagai and Raskoh respectively, representing the magmatic arc of the Makran subduction zone. The

Chagai magmatic arc extends north into Afghanistan, and comprises Cretaceous to Quaternary magmatism similar to Chagai arc (Shareq et al., 1977).

The current tectonic setting of the region, i.e., the presence of a north dipping oceanic subduction zone, an active accretionary prism followed by a magmatic arc (Chagai-Raskh) comprising subduction-related magmatism reflect a straightforward Andean-type continental margin setting. Most of the previous workers have favored this tectonic setting of origin not only for the Quaternary volcanics but also for the volcanic rocks as old as Late Cretaceous (Vredenburg, 1901; Stoneley, 1974; Nigell, 1975; Sillitoe, 1978; Dykstra, 1978; Britzman, 1979; Arthurton et al., 1979; Farah et al., 1984a, b; Arthurton et al., 1982; Kazmi and Jan, 1997). Siddiqui (1996) has contradicted this viewpoint and proposed oceanic island arc setting for the Late Cretaceous to Paleocene volcanics of the Chagai arc.

The present work is amongst the first of the systematic studies carried out on the field relations, petrography and geochemistry of the volcanic rocks of the Chagai magmatic arc. One of the principal findings of this study include the realization that whereas the Oligocene to Quaternary volcanics did form in continental margin setting, the older volcanic rocks (i.e., Late Cretaceous to Paleocene) have composition which are more appropriate for their origin in an oceanic arc environment rather than continental margin setting. In this paper we are presenting a detailed study of the Plio-Pleistocene volcanic rocks from the Chagai arc. For the first time these volcanics are studied in detail in terms their geology and petrogenesis.

2. Geological Setting

Much of the Chagai arc occurs in the western part of Pakistan. A small part of the arc also extends towards north in Afghanistan and west in Iran. The arc is 500 km long, 150 km wide and trends EW. The Chagai arc is considered as rear arc of Chagai-Raskoh arc system (Siddiqui, 1996). Quaternary alluvium and sand dunes conceal the northern frontier of the Chagai arc. Its southern margin, convex towards south, is bordered by an abrupt deep synclinal trough known as Dalbandin trough. The arc is bounded by Chaman and Harirud fault zones towards its eastern and western sides respectively. The Plio-Pleistocene volcanic rocks occur about 30 km N and NE of Nok Kundi (Fig. 1). The oldest rock unit of the Chagai arc is Late Cretaceous Sinjrani Volcanic Group, composed mainly of submarine stratified intercalations of basaltic to andesitic flows and pyroclastic rocks including agglomerate, volcanic breccia, volcanic conglomerate and tuff (Jones, 1960). Arthurton et al. (1979) assigned a Senonian age to the group, on the basis of Maastrichtian fauna present in the overlying Humai Formation and suggested a total thickness of about 10,000 m.

The Sinjrani Volcanic Group is invaded by the Chagai Intrusions during Late Cretaceous to Miocene including a varity of rock type such as granite, adamellite, granodiorite, tonalite, diorite and gabbro. The main sedimentary rock formations developed in the area include limestone and conglomerate of the Humai Formation (Late Cretaceous), shale, sandstone, siltstone and limestone intercalated with mafic lava flows and pyroclastic rocks of the Juzzak Formation (Paleo-Eocene) and Saindak Formation (Eocene). Shale, siltstone, sandstone and limestone sequence of Amalaf Formation (Oligocene to Miocene), multicoloured conglomerate, sandstone, gritstone and clays of Dalbandin Formation (Miocene-Pliocene), mottled clays, sandstone and conglomerate represent Quaternary deposits. Plio-Pleistocene lava flows and pyroclastics are known as Koh-e-Sultan Volcanic Group (Fig. 2). In Chagai arc several episodes of volcanism are identified during Late Cretaceous to Pleistocene (Jones, 1960). The Late Cretaceous volcanic activity is most wide spread and is represented by Sinjrani Volcanic Group (Jones, 1960). Later substantial volcanism occurred during Paleocene, Eocene, Oligocene, Miocene, Pliocene and Pleistocene (Fig. 2).

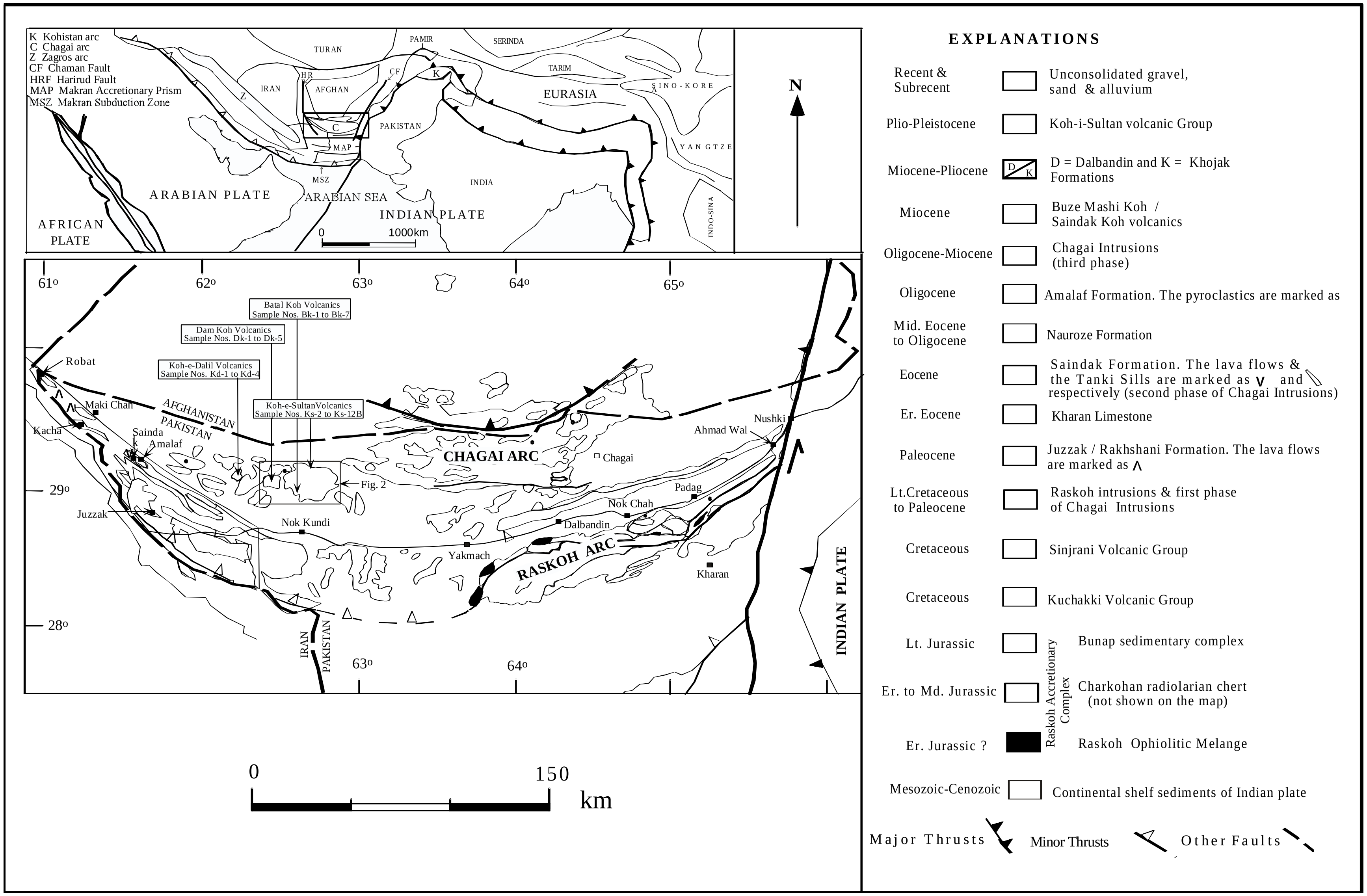

Fig. 1. Geological map of the Chagai-Raskoh arc terrane, Balochistan, Pakistan (modified and reproduced after Bakr and Jackson, 1964; Siddiqui et al., 2005).

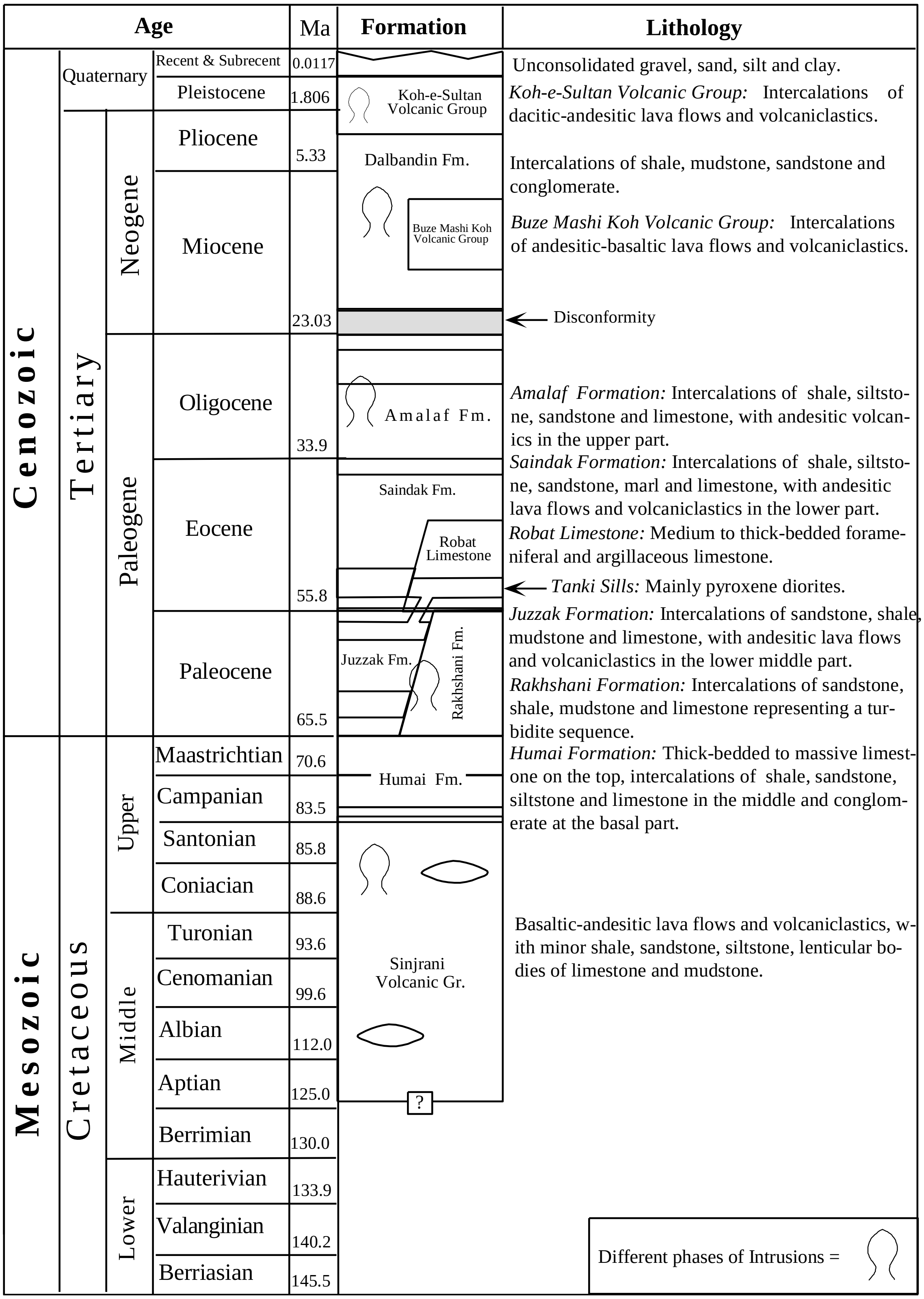

Fig. 2. Generalized stratigraphic sequence in the Chagai arc (after Jones, 1960; Siddiqui et al., 2005). The ages in the time scale are after Ogg et al. (2008).

The Plio-Pleistocene volcanic rocks, named as Koh-e-Sultan Volcanic Group (Jones, 1960), were previously considered as Quaternary (Pleistocene) in age but recent studies (Siddiqui et al., 2002; Siddiqui, 2004) have assigned a 2.39 ± 0.05 Ma (K-Ar whole rock age of the andesite) to 0.09 ± 0.01 Ma (K-Ar whole rock age of pumice) age to them. The main exposures of the Plio-Pleistocene volcanic rocks occur in Koh-e-Sultan mountain, covering 770 km^2 area (Figs. 3 and 4 A). This mountain forms a north-west trending series of three volcanoes with their discrete calderas, named Kansuri, Abu and Miri after the highest peak adjacent to or inside the volcanic caldera. The Miri volcano, 2,333 m high above mean sea level, occurs at the southwestern side of this volcanic series and is considered youngest. Ithas well developed crater walls, whereas other two volcanoes form collapse caldera and appears to be older in age. Inside the Miri Volcano is another small volcano with well-developed inner circular crater formed due to resurgent volcanic eruption (Fig. 2). The diameter of Miri Volcanic crater is 6.5 km, whereas the inner crater measures about 800 m in diameter. In the vicinity of Koh-e-Sultan volcano, a number of small satellite cone and plugs are found: Koh-e-Dalil, Chhota Dalil, Mit Koh, Dam Koh, Batal Koh, Bag Koh, Koh-e-Malik, and several other small and unnamed bodies (Figs. 1 and 2).

The Pliocene to Pleistocene volcanics are represented by andesitic to dacitic lava flows (< 10 volume %) and volcaniclastics including agglomerate, tuff, lapilly tuff, volcanic conglomerate and volcanic breccia (> 90 volume %). The Pliocene volcanics are generally dominated by andesites, whereas dacites occur as dominant phase in Pleistocene volcanics.

2.1. Andesitic lava flows

Andesitic lava flows are commonly form as 1 to 2 m thick beds interstratified with the volcaniclastics. These flows are grey to greenish grey, hard, resistant to weathering and generally form small ridges. At least five eruptive cycles are observed in the middle horizon of the southwestern flank of the Koh-e-Sultan volcano, whereas two more are observed northwest of Miri peak (Fig. 4A). These andesitic lavas are generally interrupted with tuffs and agglomerate sequence (Fig. 4A). The two cycles of andesite eruption within Miri Volcano are light grey in colour and form secondary craters. The lava flow, which occurs in the outer crater, is up to 100 m thick, whereas the inner one is up to 3 m thick. The andesites are porphyritic and show phenocrysts of pyroxene, plagioclase and hornblende in a fine-grained groundmass having the same mineral composition.

2.2. Dacitic lava flows

The dacitic lava flows generally occur as lava domes plugs and small satellite volcanoes inside and around Koh-e-Sultan Volcano. The dacitic flows are light grey to pinkish grey in colour and porphyritic in texture. Phenocrysts are mainly represented by hornblende, quartz, plagioclase and biotite and are embedded in a fine-grained groundmass having the same composition.

3. Petrography

3.1. Andesites

Under microscope, four types of andesites are identified, (a) hornblende-andesite, (b) hypersthene-andesite, (c) hornblende-hypersthene-andesite, and (d) lamprobolite-andesite. The main textures exhibited by the andesites are hypocrystalline and porphyritic. Other textures include cumulophyric, vitrophyric and intersetal. The main primary minerals include plagioclase, clinopyroxene, orthopyroxene, amphibole and minor quartzdescribed as under:

Plagioclase: Plagioclase crystals are euhedral to subhedral, lathlike and columnar in shape, and exhibit polysynthetic twinning (according to the albite and occasionally to the combined albite and Carlsbad laws) and oscillatory zoning. The plagioclase generally ranges in composition from An_{26} to $An_{48,}$ (oligoclase to andesine).

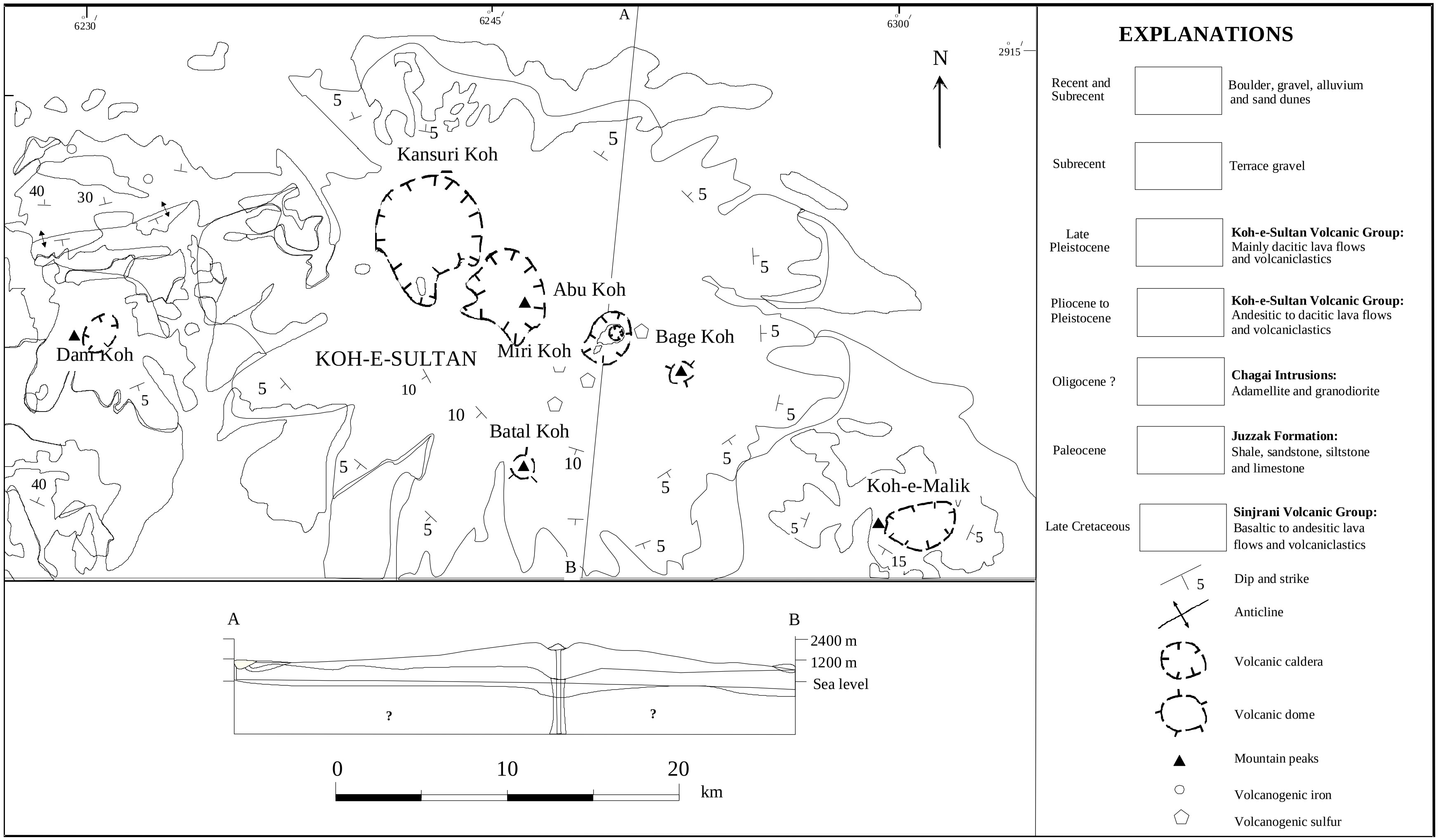

Fig. 3. Geological map of Koh-e-Sultan area (modified after Jones, 1960; Siddiqui, 2004).

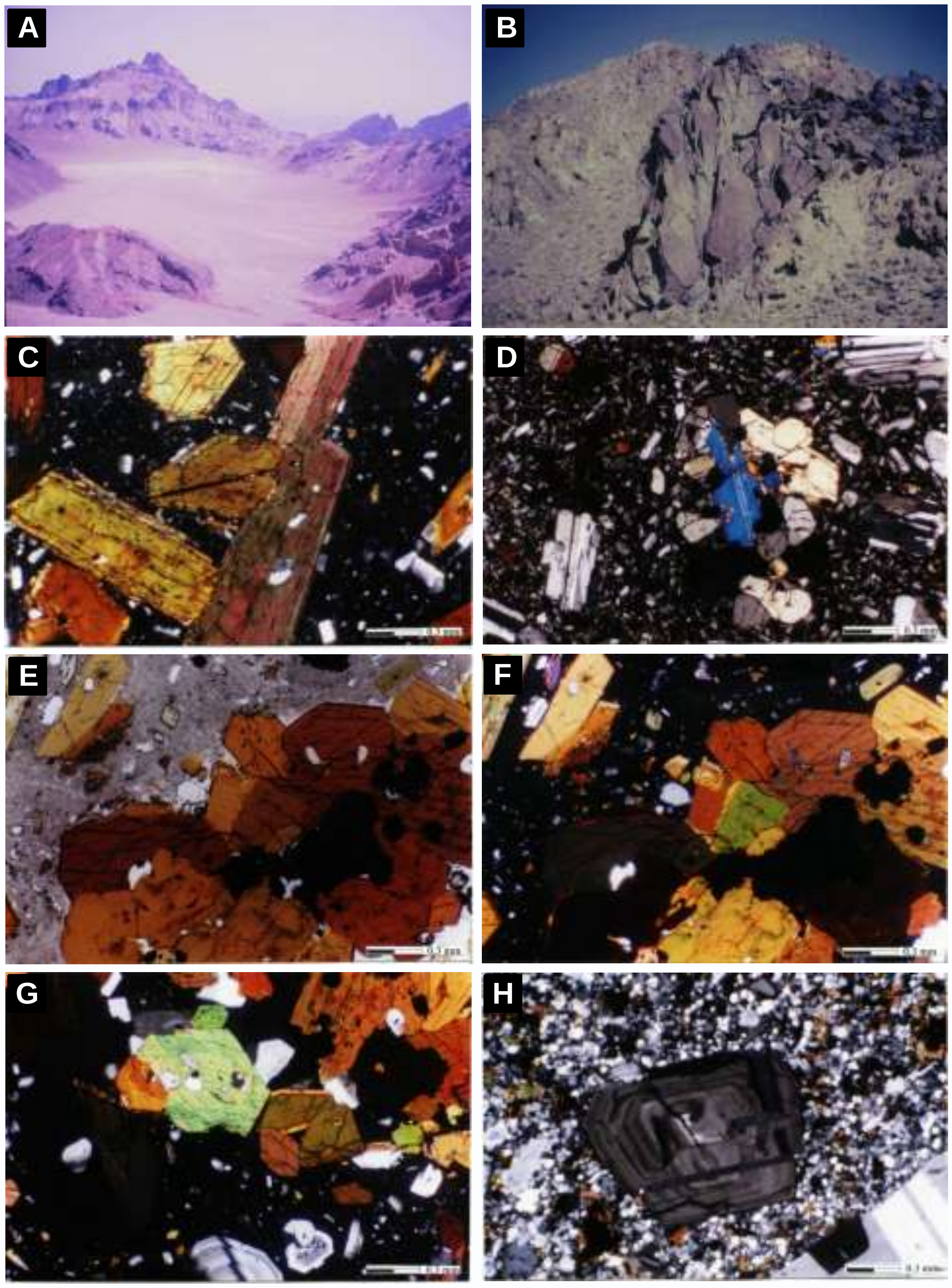

Fig. 4. (A) a view of the northern part of the Miri crater of the Koh-e-Sultan volcano, (B) andesitic lava flows intercalated with volcaniclastic rocks on the southern flank of the same volcano, (C) photomicrograph (KS-4) displaying large prismatic and polygonal phenocrysts and fragments of hornblende within a cryptocrystalline to glassy groundmass. (D) photomicrograph (KS-21) exhibiting cumulophyric texture developed by the clustering of the hypersthene phenocrysts, (E) photomicrograph (KS-5) displaying cumulophyric texture formed by clustering of lamprobolite phenocrysts in a microcrystalline to glassy groundmass (in plane polarized light), (F) the same photomicrograph in crossed polarized light. (G) photomicrograph (KS-20) displaying phenocryst of hornblende with well developed 124°-56° cleavage and small anhedral inclusions of quartz (in centre). Note strong zoning in some plagioclase crystals. Hornblede in top right contains magnetite inclusions, (H) photomicrograph of dacite (KS-9) exhibiting twining and oscillatory zoning in a phenocryst of plagioclase.

At places zoned plagioclase crystals contain abundant fluid inclusions parallel to zoning towards their margins. A few of them show resorbed and pitted margins. Larger plagioclase phenocrysts have small prismatic and polygonal inclusion of hornblende. Groundmass plagioclase generally occurs as small microlites, crystallites, and tiny columnar laths.

Pyroxene: The pyroxene is mainly represented by both, ortho- and clinohypersthene, occurring as small euhedral to subhedral prismatic crystals and square or equant basal sections. Orthopyroxene phenocrysts occasionally show green to pale brown pleochroism and exhibit polysynthetic twinning and locally developed reaction rims of hornblende. The groundmass hypersthene occurs as tinny prismatic crystals and globules in the interstices between the small plagioclase crystals, imparting to the rock a sub-intersertal texture. *Amphibole:* The amphibole is mainly represented by hornblende with substantial oxy- hornblende. Hornblende shows yellowish green to green and lamprobolite light brown to reddish brown pleochroism, whereas both displays well developed sets of 56° and 124° cleavages in basal sections. It occurs as large euhedral prismatic grains and polygonal basal sections, occasionally showing polysynthetic twinning (Fig. 4C). Some of the amphibole crystals exhibit a rim of abundant fluid inclusions as in the case of plagioclase. The lamprobolitee crystals generally occur in clusters imparting to the rocks a cumulophyric texture (Fig. 4E & F). In the groundmass lamprobolitee occurs as small prismatic crystals and tinny polygonal basal sections.

Quartz: It generally occurs as small subhedral and equant phenocrysts.

Volcanic Glass: The volcanic glass is commonly devitrified and has brown colour, which generally occurs in groundmass and as fillings in vesicles.

Accessory Minerals: These includeapatite, magnetite,pyrite and chalcopyrite. Apatite occurs as small euhedral and prismatic crystals enclosed in larger grains of plagioclase. Magnetite occurs as small subhedral to anhedral crystals scattered throughout the groundmass. The pyrite and chalcopyrite are found as small anhedral and irregular grains.

Secondary Minerals: Secondary minerals are developed as partial or complete replacement of primary minerals. At places, pyroxene and hornblende are partially altered into chlorite. Clay mineral, sericite, and calcite have developed after partial alteration of plagioclase. Magnetite is partially to completely replaced by hematite, but occasionally by limonite.

3.2. Dacite

The dacite is represented by only one variety: hornblende dacite. These rocks (KS-6 & KS-9) are holocrystalline porphyritic and cumulophyric in texture. Large phenocrysts (0.1 - 7.0 mm) of plagioclase and amphibole are embedded in a microcrystalline groundmass having the same minerals. The phenocryst groundmass ratio is 45:55.

Plagioclase: Plagioclase crystals are euhedral to subhedral, lathlike, columnar and equant in shape and exhibit polysynthetic twinning according to the albite and occasionally to the combined albite and Carlsbad laws. The anorthite contents of plagioclase could not be determined due to the development of strong oscillatory zoning in all phenocrysts (Fig. 4H). At places zoned plagioclase crystals have abundant fluid inclusions towards their margins parallel to zoning planes. Larger plagioclase phenocrysts have small tabular and lathlike inclusion of earlier generation of plagiclase itself. Groundmass plagioclase generally occurs as small anhedral and equant crystals and tiny columnar laths.

Quartz: It generally occurs as small subhedral and equant phenocrysts and microcrystalline anhedral and equant crystals in the groundmass. Quartz is also found as anhedral inclusions in hornblende.

Amphibole: The amphibole is mainly represented by brownish green hornblende. It shows yellowish green to brownish green pleochroism and two sets of well-developed cleavages in basal sections. The hornblende generally occurs as large euhedral prismatic grains and polygonal basal sections, which occasionally show polysynthetic twinning. Some of the hornblende crystals exhibit a rim of abundant fluid inclusions towards their margin as in the case of plagioclase.

Biotite: The biotite generally forms small prismatic lamellae or flaky aggregates in the groundmass.

Accessory Minerals: Mainly apatite and magnetite with substantial pyrite and chalcopyrite are included in accessories. Apatite occurs as small euhedral and prismatic crystals enclosed in larger grains of plagioclase. Magnetite occurs as small subhedral to anhedral crystals scattered throughout the groundmass. Pyrite and chalcopyrite are found as small anhedral and irregular grains.

Secondary Minerals: Some hornblende is partially altered into biotite and chlorite. Clay mineral, sericite, and calcite have developed after partial alteration of plagioclase. Magnetite is partially to completely replaced by hematite and the later is altered into limonite.

4. Geochemistry

A total number of 29 rock samples were collected from the Plio-Pleistocene volcanics of the Chagai arc. Out of these, 13 (Ks-2 to 8A & Ks-8B to12A & 12B) were collected from Koh-e-Sultan (KSV) volcano area, seven (Bk-1 to 7) from Batal Koh (BKV), five (Dk-1 to 5) from Dam Koh (DKV) and four (Kd-1 to 4) from Koh-e-Dalil (KDV). All the samples are analyzed for major and trace elements. Five samples from Koh-e-Sultan area are also analyzed for rare earth elements (REE).

4.1. Analytical Techniques

4.1.1. Major and Trace Elements Analyses

The major and trace elements were analyzed in the Geoscience Laboratory, Geological Survey of Pakistan, Islamabad, by X-ray fluorescence spectrometry (RIGAKU XRF-3370E). The sample powder (<200 mesh), weighing 0.7 gram was thoroughly mixed with 3.5 gram of lithium tetra borate (flux). The analyses were carried out on 1:5 rock powder and flux fused disks commonly known as glass beads. The samples thus obtained were analyzed by XRF using corresponding GSJ (Geological Survey of Japan) standard samples with every batch of ten samples. The results of analyses were then compared with the recommended values of USGS (United State Geological Survey) standard reference samples. A check of precision of the instrument was made using JA-3 standard sample (Govindaraju, 1989).

4.1.2. Rare Earth Elements Analyses:

Rare earth elements (REE) and Hf, Th, U and Ta were analysed in the GSJ using ICP-MS 2000 (YOKOGAVA, Japan). About 200 g of powdered sample (< 200 mesh) was weighed in a platinum dish and 3 ml $HClO_4$, 4 ml HNO_3 and 5 ml HF was added to the sample. The sample was then heated on the hot plate at 200°C till complete evaporation. The dish was removed from the hot plate, cooled, washed and dried. The residue was added 5 ml 1:1 HNO_3 and 5 ml water and gently heated on the hot plate till complete dissolution. The solution in the dish was cooled and filtered. The filtrate was transferred into a 100 ml measuring flask and added water up to 100 ml mark. The solution thus obtained was analyzed by ICP-MS, following Imai (1990) method, using JB-1 and JA-1 as standard samples (Govindaraju, 1989) and 1.5% HNO_3 as blank sample. The detection limits of ICP-MS 2000 for all these elements are < 0.1 ppm. A check of precision of the instrument was made using JB-1 and JA-1 standard samples (Govindaraju, 1989).

4.2. Major Element Abundances

Bulk chemical analyses of samples from these volcanics are given in Table 1. The major elements are recalculated on a volatile free basis, because a few of the samples show loss on ignition up to 1.49 wt. % due to alteration.

Table 1. Bulk chemistry of Plio-Pleistocene volcanic rocks from the Chagai arc.

Elements & Ratios	Koh-e-Sultan Volcanics									
	Ks-2	Ks-3	Ks-5	Ks-6	Ks-7	Ks-8	Ks-8b	Ks-9	Ks-11	Ks-12b
SiO_2	58.34	59.12	63.08	61.42	63.49	61.34	62.76	61.67	63.05	63.36
TiO_2	0.64	0.49	0.46	0.46	0.44	0.53	0.48	0.53	0.47	0.43
Al_2O_2	16.97	15.51	17.02	17.09	17.16	17.55	17.1	17.23	17.14	17.15
Fe_2O_3	6.93	6.68	4.85	5.11	4.63	5.16	4.85	5.21	4.85	4.6
MnO	0.13	0.33	0.1	0.15	0.1	0.15	0.15	0.1	0.1	0.1
MgO	4.8	5.9	3.01	3.25	2.77	3.32	3.01	3.39	2.98	2.75
CaO	6.95	5.81	6.2	7.34	6.14	6.83	6.27	6.67	6.04	6.19
Na_2O	3.92	4.72	4.09	4.07	4.15	4.03	4.24	4.09	4.2	4.25
K_2O	1.15	1.28	1.04	0.97	0.97	0.95	1.01	0.97	0.99	1.02
P_2O_5	0.16	0.16	0.14	0.14	0.13	0.13	0.13	0.13	0.13	0.13
FeOt/MgO	1.28	1.01	1.43	1.40	1.49	1.38	1.43	1.37	1.45	1.49
K_2O/Na_2O	0.29	0.27	0.25	0.24	0.23	0.24	0.24	0.24	0.24	0.24
Mg #	58	64	55	56	55	56	55	57	55	55
Rb	26	34	19	18	19	22	21	22	19	18
Sr	429	433	493	482	494	471	475	463	479	490
Ba	300	338	436	362	443	351	434	419	423	421
V	151	116	98	123	96	141	91	149	100	89
Cr	261	205	42	87	92	111	28	120	38	100
Co	26	20	33	18	16	20	50	19	31	15
Ni	68	19	16	20	17	18	12	19	13	16
Zr	99	97	75	75	71	71	69	72	74	72
Y	16	13	12	12	12	14	12	13	12	12
Nb	4	4	4	3	4	4	3	3	3	4
Hf	0.6	0.36	—	—	—	—	—	1.31	—	—
Ta	0.18	0.19	—	—	—	—	—	0.24	—	—
Th	2.93	1.74	—	—	—	—	—	2.12	—	—
U	0.61	0.44	—	—	—	—	—	0.66	—	—
Sc	21	15	16	21	20	26	16	27	20	17
La	15.15	13.01	—	—	—	—	—	10.02	—	—
Ce	27.63	25.11	—	—	—	—	—	19.76	—	—
Nd	13.43	11.53	—	—	—	—	—	8.94	—	—
Sm	2.66	2.25	—	—	—	—	—	1.92	—	—
Eu	1	0.79	—	—	—	—	—	0.68	—	—
Gd	3.54	2.21	—	—	—	—	—	2.14	—	—
Er	1.23	0.99	—	—	—	—	—	1.11	—	—
Yb	1.67	1.03	—	—	—	—	—	1.14	—	—
∑REE	66.31	56.92	—	—	—	—	—	45.71	—	—
Eu_N/Eu^*	1	1.09	—	—	—	—	—	1.03	—	—
Ce_N/Ce^*	1.02	1.08	—	—	—	—	—	1.1	—	—
$(La/Yb)_N$	6.05	8.42	—	—	—	—	—	5.86	—	—
$(Ce/Yb)_N$	4.21	6.2	—	—	—	—	—	4.41	—	—
$(La/Sm)_N$	3.5	3.56	—	—	—	—	—	3.21	—	—
$(La/Ce)_N$	1.44	1.36	—	—	—	—	—	1.33	—	—
Th/Yb	1.75	1.69	—	—	—	—	—	1.86	—	—
Ta/Yb	0.11	1.18	—	—	—	—	—	0.21	—	—
La/Yb	9.07	12.63	—	—	—	—	—	8.79	—	—
Ce/Yb	41.24	24.38	—	—	—	—	—	17.33	—	—
Zr/Y	6.19	7.46	6.25	6.25	5.92	5.07	5.75	5.54	6.17	6.00
Zr/Nb	24.75	24.25	18.75	25.00	17.75	17.75	23.00	24.00	24.67	18.00
Ti/Zr	38.72	30.26	36.74	36.74	37.12	44.71	41.67	44.09	38.04	35.77
Ti/V	25.39	25.30	28.12	22.40	27.45	22.52	31.60	21.31	28.15	28.94

FeOt = Total iron as FeO, Mg # =100xMg /Mg+Fe^{+2}, SiO_2-P_2O_5 are in %, Rb-Yb are in ppm. REE ratios with $_N$ are chondrite normalized
(after Nakamura, 1974), REE with * are interpolated values (see text for details).

Table 1. Continued

Elements & Ratios	Koh-e-Sultan Volcanics			Batal Koh Volcanics						
	Ks-4	Ks-10	Ks-12a	Bk-1	Bk-2	Bk-3	Bk-4	Bk-5	Bk-6	Bk-7
SiO_2	63.55	63.89	64.83	59.6	59.53	59.36	59.64	59.14	57.49	57.45
TiO_2	0.44	0.44	0.42	0.58	0.59	0.59	0.58	0.59	0.64	0.64
Al_2O_2	17.12	17.14	17.03	17.83	17.84	18.05	17.8	17.81	18.47	18.45
Fe_2O_3	4.7	4.57	4.36	6.09	6.18	6.29	6.24	6.23	6.88	6.78
MnO	0.1	0.1	0.1	0.12	0.12	0.13	0.12	0.12	0.13	0.13
MgO	2.86	2.74	2.55	3.38	3.29	3.4	3.43	3.35	3.46	3.4
CaO	5.22	5.68	5.39	7.18	7.27	7.07	6.91	7.21	7.98	8.34
Na_2O	4.23	4.27	4.27	4.11	4.05	4.08	4.22	4.03	3.86	3.75
K_2O	1.01	1.04	0.92	0.92	0.93	0.84	0.88	0.88	0.88	0.84
P_2O_5	0.13	0.12	0.13	0.18	0.19	0.19	0.18	0.19	0.21	0.21
FeOt/MgO	1.46	1.48	1.52	1.60	1.67	1.64	1.62	1.65	1.77	1.77
K_2O/Na_2O	0.24	0.24	0.22	0.22	0.23	0.21	0.21	0.22	0.23	0.22
Mg #	55	56	55	53	52	52	52	52	50	50
Rb	19	19	29	18	18	14	17	18	16	15
Sr	489	474	490	504	508	513	530	509	519	564
Ba	419	406	502	365	368	414	362	320	314	353
V	109	97	91	99	108	90	87	95	126	131
Cr	102	33	27	64	85	45	123	45	65	44
Co	16	32	36	16	18	32	19	36	19	22
Ni	18	13	14	15	17	19	21	18	12	12
Zr	73	71	75	113	112	115	112	108	101	101
Y	11	12	11	16	16	16	16	16	16	17
Nb	4	3	3	5	4	4	4	4	4	4
Hf	1.39	—	—	17	17	17	20	16	17	20
Ta	0.18	—	—	1.13	1.13	0.88	1.06	1.13	1.00	0.88
Th	3.02	—	—	22.81	23.00	25.88	22.63	20.00	19.63	20.76
U	1.02	—	—	3.23	3.29	3.60	3.23	2.96	3.11	3.50
Sc	19	26	22	7.06	7.00	7.19	7.00	6.75	6.31	5.94
La	15.90	—	—	22.60	28.00	28.75	28.00	27.00	25.25	25.25
Ce	28.17	—	—	30.75	31.55	30.73	31.02	32.72	37.96	37.96
Nd	12.58	—	—	35.09	32.72	39.27	39.93	37.20	30.43	29.26
Sm	1.98	—	—	424	429	498	430	406	457	465
Eu	0.91	—	—	20.92	20.98	16.84	20.18	22.83	23.26	19.75
Gd	3.16	—	—	0.036	0.035	0.027	0.032	0.035	0.031	0.027
Er	1.02	—	—	28	28	37	31	28	32	38
Yb	1.34	—	—	0.31	0.25	0.25	0.25	0.25	0.25	0.24
∑REE	65.06	—	—	1.13	1.00	0.89	0.95	0.89	1.42	1.67
Eu_N/Eu^*	1.12	—	—	—	—	—	—	—	—	—
Ce_N/Ce^*	1.05	—	—	—	—	—	—	—	—	—
$(La/Yb)_N$	7.91	—	—	—	—	—	—	—	—	—
$(Ce/Yb)_N$	5.35	—	—	—	—	—	—	—	—	—
$(La/Sm)_N$	4.94	—	—	—	—	—	—	—	—	—
$(La/Ce)_N$	1.48	—	—	—	—	—	—	—	—	—
Th/Yb	2.25	—	—	—	—	—	—	—	—	—
Ta/Yb	0.13	—	—	—	—	—	—	—	—	—
La/Yb	11.87	—	—	—	—	—	—	—	—	—
Ce/Yb	21.02	—	—	—	—	—	—	—	—	—
Zr/Y	6.64	5.92	6.82	7.06	7.00	7.19	7.00	6.75	6.31	5.94
Zr/Nb	18.25	23.67	25.00	22.60	28.00	28.75	28.00	27.00	25.25	25.25
Ti/Zr	36.10	37.12	33.54	30.75	31.55	30.73	31.02	32.72	37.96	37.96
Ti/V	24.18	27.17	27.65	35.09	32.72	39.27	39.93	37.20	30.43	29.26

FeOt = Total iron as FeO, Mg # =100xMg /Mg+Fe^{+2}, SiO_2-P_2O_5 are in %, Rb-Yb are in ppm. REE ratios with $_N$ are chondrite normalized (after Nakamura, 1974), REE with * are interpolated values (see text for details).

Table 1. Continued

Elements & Ratios	Dam Koh Volcanics					Koh-e-Dalil Volcanics			
	Dk-1	Dk-2	Dk-3	Dk-4	Dk-5	Kd-1	Kd-2	Kd-3	Kd-4
SiO_2	60.15	61.55	60.98	63.16	63.76	57.98	58.12	59.87	59.37
TiO_2	0.51	0.52	0.54	0.48	0.49	0.7	0.71	0.61	0.61
Al_2O_3	17.4	17.97	17.83	17.22	17.01	17.76	17.93	17.6	17.41
Fe_2O_3	5.45	5.47	5.58	4.88	4.65	6.47	6.49	5.72	5.74
MnO	0.1	0.12	0.11	0.1	0.1	0.11	0.11	0.1	0.1
MgO	3.24	2.43	2.89	2.57	2.6	4.11	3.99	3.51	3.59
CaO	7.96	6.37	6.36	5.95	5.65	7.76	7.6	7.2	8.16
Na_2O	4.25	4.43	4.36	4.21	4.24	3.78	3.72	3.87	3.78
K_2O	0.78	0.94	1.11	1.26	1.33	1.12	1.14	1.18	1.09
P_2O_5	0.17	0.2	0.24	0.17	0.18	0.2	0.19	0.26	0.16
FeOt/MgO	1.50	2.00	1.72	1.69	1.59	1.42	1.46	1.48	1.44
Na_2O/K_2O	5.45	4.71	3.93	3.34	3.19	3.38	3.26	3.28	3.47
K_2O/Na_2O	0.18	0.21	0.25	0.30	0.31	0.30	0.31	0.30	0.29
Mg #	54	47	51	51	53	—	—	—	—
Ti	3055	3115	3235	2875	2935	4193	4253	3654	3654
K	6474	7802	9213	10458	11039	9296	9462	9794	9047
P	741	872	1046	741	785	872	828	1134	698
Rb	16	21	31	31	30	16	16	18	17
Sr	590	523	545	619	591	917	890	857	855
Ba	369	375	423	661	608	410	398	425	423
V	112	105	105	84	96	201	195	183	170
Cr	74	54	115	43	56	32	33	33	35
Co	19	16	18	13	14	21	19	12	20
Ni	21	7	18	13	14	14	13	12	12
Zr	92	128	124	96	98	113	113	112	109
Y	12	15	15	12	12	13	14	13	12
Nb	4	5	7	6	7	4	4	4	4
Sc	17	12	15	14	16	28	26	22	23
Rb/Y	1.33	1.40	2.07	2.58	2.50	1.23	1.14	1.38	1.42
Ba/Y	30.75	25.00	28.20	55.08	50.67	31.54	28.43	32.69	35.25
Ba/Zr	4.01	2.93	3.41	6.89	6.20	3.63	3.52	3.79	3.88
Zr/Y	7.67	8.53	8.27	8.00	8.17	8.69	8.07	8.62	9.08
Zr/Nb	23.00	25.60	17.71	16.00	14.00	28.25	28.25	28	27.25
Ti/Zr	33.21	24.33	26.09	29.95	29.95	37.11	37.64	32.63	33.52
Ti/V	27.28	29.66	30.81	34.23	30.57	20.86	21.81	19.97	21.49
K/Rb	405	372	297	337	368	581	591	544	532
K/Ba	17.54	20.81	21.78	15.82	18.16	22.67	23.77	23.04	21.39
Rb/Sr	0.027	0.040	0.057	0.050	0.051	0.017	0.018	0.021	0.020
Sr/Rb	37	25	18	20	20	57.31	55.63	47.61	50.29
Nb/Y	0.33	0.33	0.47	0.50	0.58	0.31	0.29	0.31	0.33
Sc/Ni	0.81	1.71	0.83	1.08	1.14	2.00	2.00	1.83	1.92

FeOt = Total iron as FeOt, Mg # =100xMg /Mg+Fe^{+2}, SiO_2-P_2O_5 are in %, Rb-Yb are in ppm

All the rock samples collected from Plio-Pleistocene volcanics are classified according to the TAS (total alkali silica) classification of IUGS and are plotted in SiO_2 versus alkali (wt. %) diagrams (Fig. 5) of Le Bas et al. (1986). In this diagram, 22 samples plot in andesite fields, whereas five from Koh-e-Sultan area and two from Dam Koh area plot in dacite field or just on boundary between andesite and dacite fields. All the samples from Plio-Pleistocene volcanics are also plotted in K_2O versus SiO_2 diagrams (after Gill, 1981). In this diagram samples plot in midium to low-K.andesite and dacite fields (Fig. 6).

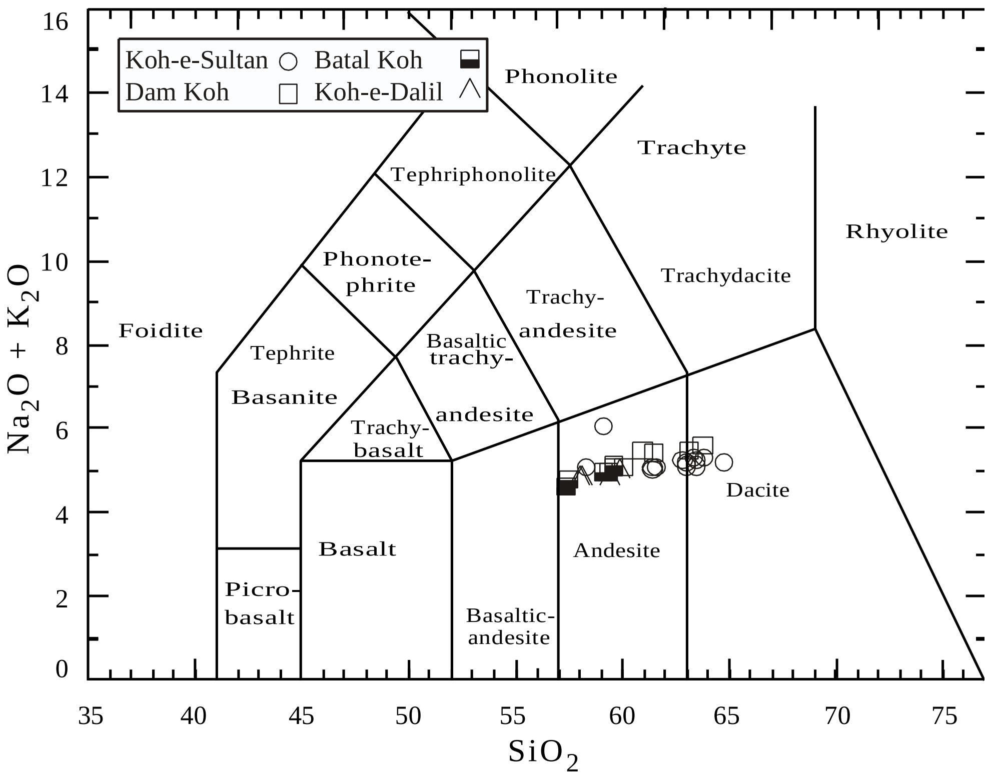

Fig. 5. Alkali versus SiO_2 plot (after Le Bas, *et al.*, 1986) for the Plio-Pleistocene volcanic rocks from the Chagai arc.

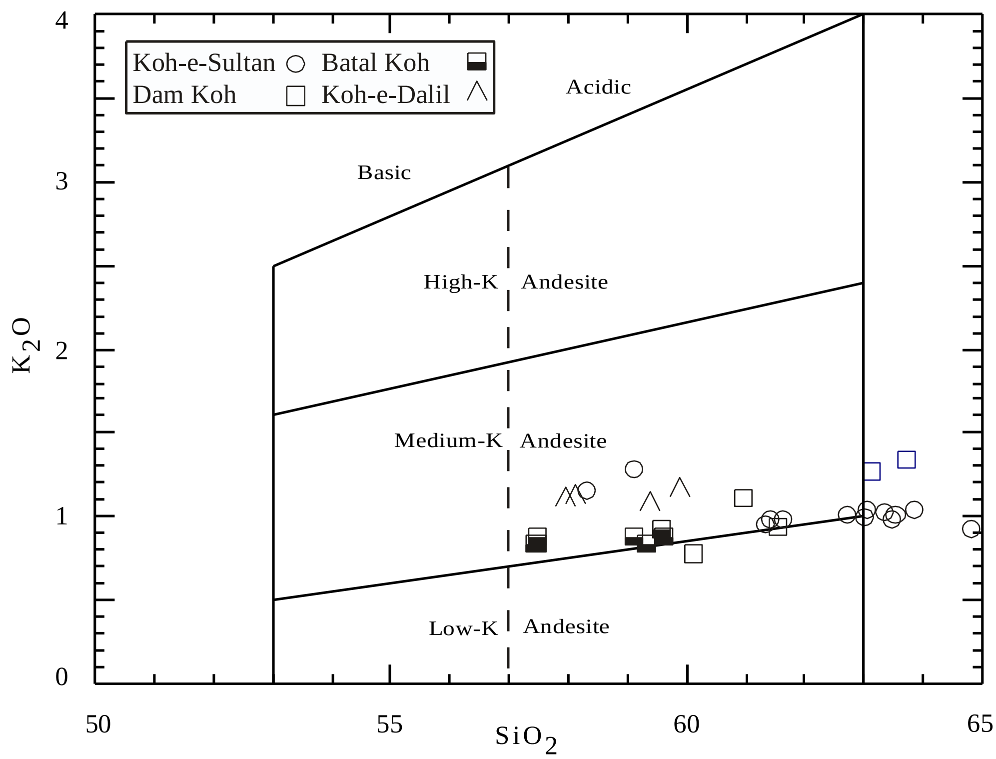

Fig. 6. K_2O versus SiO_2 diagram (after Gill, 1981) for the Plio-Pleistocene volcanic rocks from the Chagai arc.

The SiO_2 contents in KSV have a wider range (58.35-64.83 wt. %), as compared to others BKV (57.45-59.64 wt. %), KDV (57.98-59.87 wt. %), DKV (61.15-63.16 wt. %). The TiO_2, Al_2O_3, Fe_2O_3, CaO and P_2O_5 contents (Table 1) are within the proposed range of most orogenic andesites (Gill, 1981). The volcanics have lower but greatly variable (2.55-4.80) range for MgO wt. %, except one andesite sample from KSV shows higher value (5.90) for MgO wt. %, which is little lower than high-Mg andesite value (> 6 wt. % MgO) proposed by Gill (1981). The KDV have lower and narrow overlapping range for Na_2O (3.72-3.87 wt. %) and K_2O (1.09-1.18 wt. %). All other volcanics have a wider and variable range (Table 1). The K_2O/Na_2O ratios in all the volcanic are low (0.18-0.31), which are much lower than the reported (0.60-1.00) ratios for common continental margin type arcs. The KDV have narrow and lower (1.42-1.1.48) FeOt/MgO ratios as compared to all other volcanics, which have a wider and higher overlapping range (1.01-2) for this ratio. All the volcanics show a lower and narrow (47-58) range for Mg # (100 × Mg/Mg + Fe^{2+}), which are consistent with most volcanic rocks of orogenic arcs (Gill, 1981).

4.3. Major Element Variations

SiO_2 is used as fractionation index in various Harker-type variation diagrams for major elements (Fig. 7). In these diagrams, almost all the samples from the area show sharp to scattered negative correlation for Al_2O_3, MgO, Fe_2O_3, TiO_2, CaO and P_2O_5. The negative correlation for MgO, Fe_2O_3, and TiO_2 are due to the early fractionation of pyroxene, hornblende and magnetite. The similar trends for Al_2O_3 and CaO are probably due to fractionation of plagioclase. The P_2O_5 exhibit a scattered negative correlation, due probably to fractionation of apatite. Na_2O and K_2O show scattered positive correlation with SiO_2 probably due to the enrichment of these elements in the residual phase.

4.4. Trace Element Variations

MgO is used as fractionation index in various Harker-type variation diagrams for trace elements (Fig. 8). The analysis show scattered negative correlation for Ba, and Rb (except BVC) due to the enrichment of these elements in the residual phase. Ti, V, Sc, P, Co and Ni exhibit sharp to scattered positive correlation (except BVC) for all the volcanics probably due to the partitioning of these elements in magnetite, apatite, hornblende and pyroxene during differentiation. In all the diagrams BVC show nonsystematic behavior, probably due to limited MgO concentration.

4.5. Trace element abundances

Large Ion Lithophile Elements (LILE): The volcanics generally have higher abundances of LILE as compared to high field strength elements (HFSE). The KDV volcanics generally have lower abundances and narrow range for Rb (16-18 ppm), Sr (855-917 ppm) and Ba (398-410 ppm). The other volcanics have a wider and variably higher overlapping range for Rb (14-34 ppm), Sr (433-619 ppm) and higher for Ba (300-661 ppm), which are consistent with the calc-alkaline volcanic rocks of orogenic arcs (Gill, 1981). Th and U, analyzed only in the KSV, range from 1.74 to 3.02 ppm and 0.44 to 1.02 ppm, respectively.

High Field Strength Elements (HFSE): The KSV volcanics generally have lower abundances of Zr (69-99 ppm), Nb (3-4 ppm) and Y (11-16 ppm). The other volcanics have higher overlapping abundances for these elements. Zr, 92 to 113 ppm, Nb 4 to 7 ppm, and and Y 12 to 17 ppm, respectively, which suggest that KSV volcanics were formed by relatively higher degree of partial melting as compared to the other volcanics. The concentration of HFSE in these volcanics is consistent with an enriched sub-arc mantle peridotite source and corresponds to calc-alkaline volcanic rocks of orogenic arcs (Gill, 1981). Ta and Hf were analyzed only in KSV, andrange from 0.18 to 0.24 ppm and 0.36 to 1.39 ppm, respectively.

Compatible Elements: The KSV volcanics have a variable and higher overlapping range for Cr (27-261 ppm), Ni (13-68 ppm), Co (15-50 ppm), V (89-151 ppm), and Sc (15-27 ppm). The other volcanics have lower but greatly variable overlapping range of compatible elements: Cr (33-123 ppm), Ni (12-21 ppm), Co (12-36 ppm), V (84-201 ppm) and Sc (84-201 ppm). These values are much lower than the values proposed (Gill, 1981) for the volcanic rocks of orogenic arcs that are directly derived from the primary mantle source.

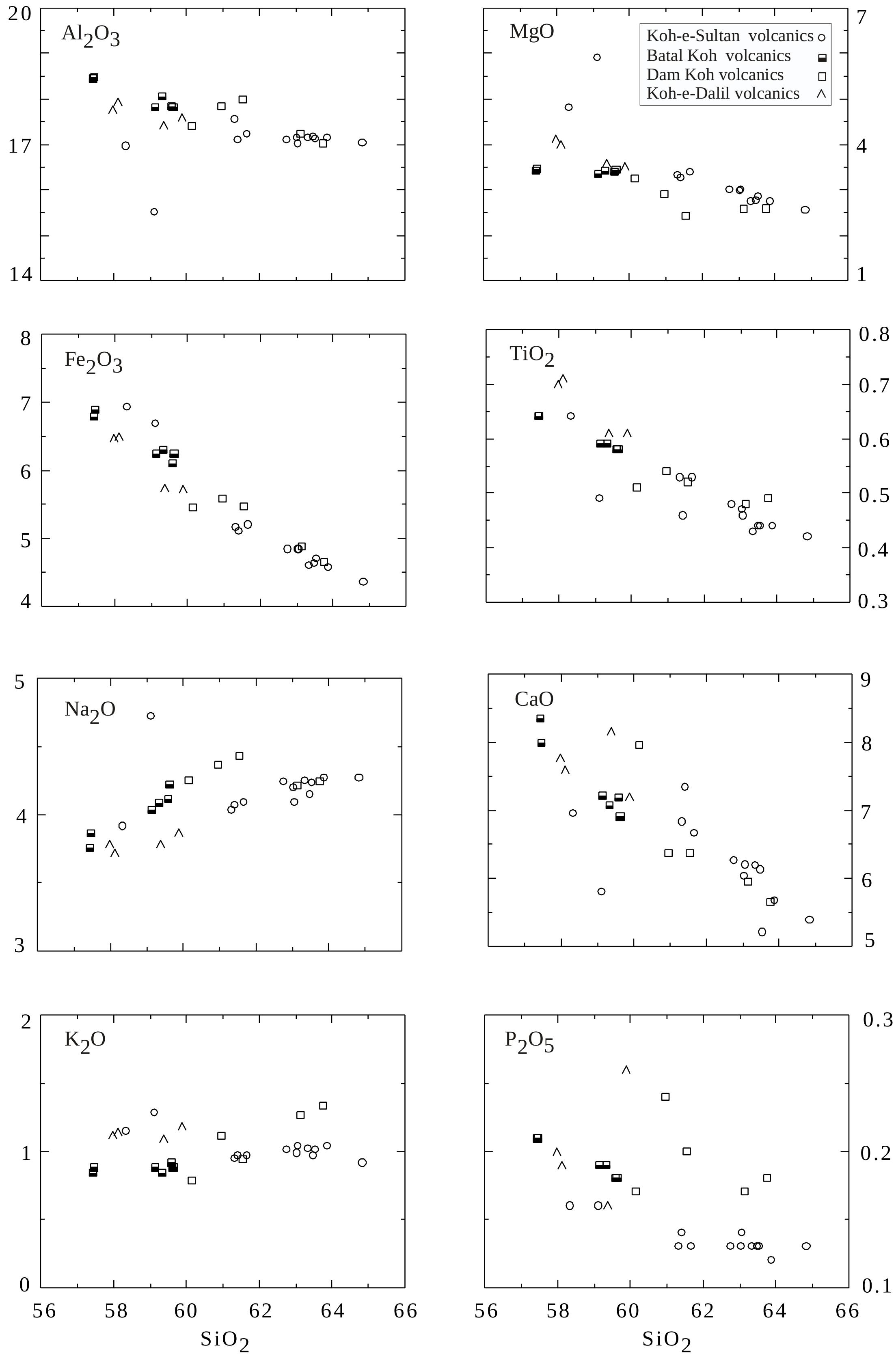

Fig. 7. Harker type variation diagrams for major elements showing fractionation trends in the Plio-Pleistocene volcanic rocks of the Chagai arc

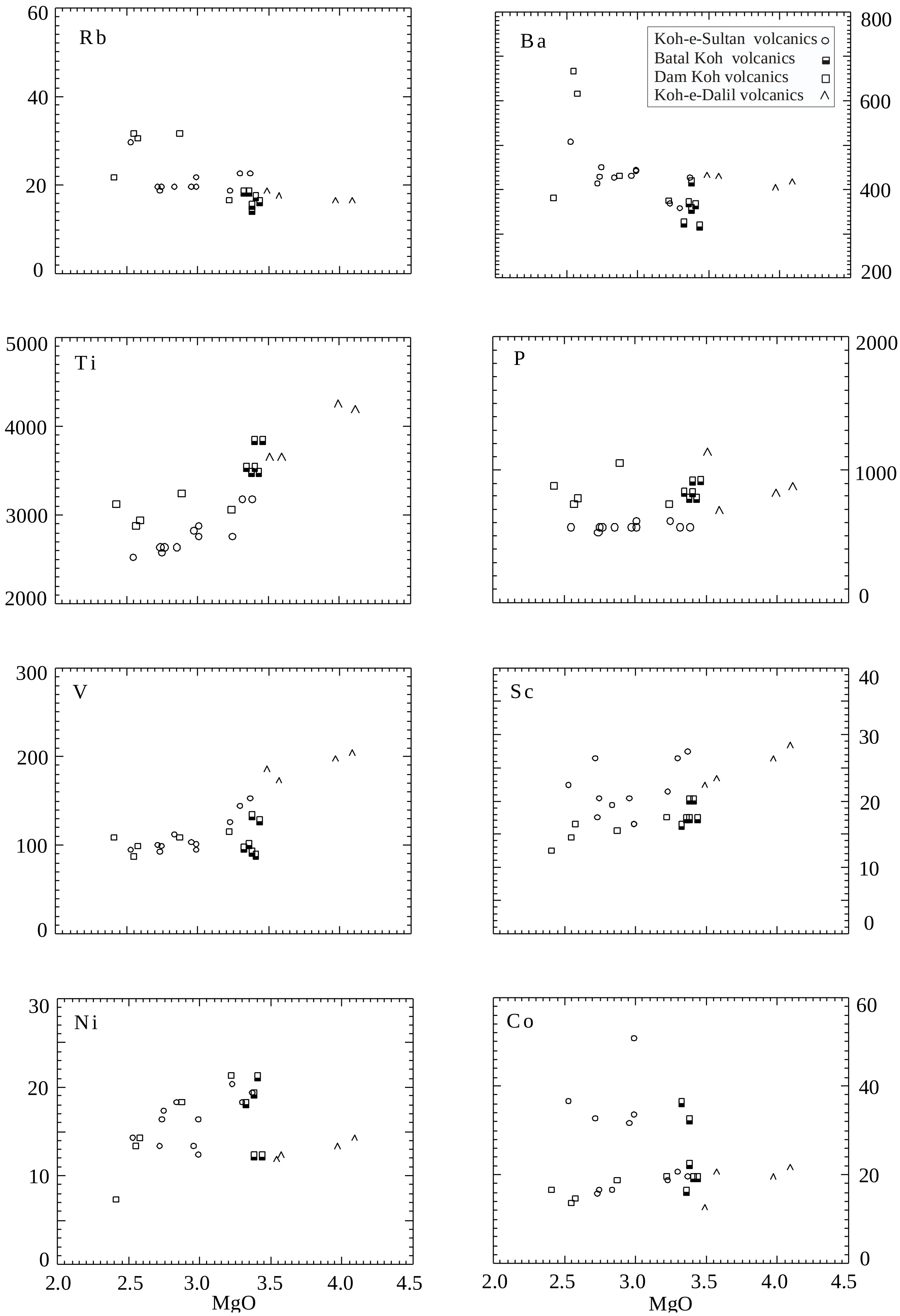

Fig. 8. Harker type variation diagrams for trace elements showing fractionation trends in the Plio-Pleistocene volcanic rocks of the Chagai arc.

Rare Earth Elements (REE): The rare earth elements (La, Ce, Nd, Sm, Eu, Gd, Er & Yb) were analyzed in only in four samples from KSV (Ks-2, 3, 4 & 9) Plio-Pleistocene volcanics. The total REE concentration is moderate and ranges from 45.71 to 66.31. The volcanics generally have rather higher normalized LREE/HREE ratios (La_N/Yb_N = 5.86-8.42, Ce_N/Yb_N = 4.21-6.20), which suggests that they are derived from a LREE enriched mantle peridotite source. The rocks have very narrow range of La_N/Ce_N (1.33-1.48) and La_N/Sm_N (3.21-4.94) ratios, which suggests that all the volcanics of KSV had a uniform mantle source. The measured Eu anomalies (Eu_N/ Eu*), which are calculated by dividing the chondrite normalized (Eu_N) values and the interpolated (Eu*) values [$Eu_N/Eu^* = Eu_N/\sqrt{(Sm_N \times Gd_N)}$]. (Taylor & McLennan, 1985)have values very close to one (1.03 to 1.12). Similarly, measured Ce anomalies (Ce_N/Ce^*), which are calculated by dividing the chondrite normalized (Ce_N) values with the interpolated (Ce*) values [$Ce_N/Ce^* = Ce_N/\sqrt{(La_N \times Nd_N)}$] have positive values, which negate the involvement of subducted pelagic sediments in their magma generation (Hole et al., 1984).

Spider Diagrams: The spider diagrams or multi-elements diagram are generally used to study the behavior of incompatible trace elements in the rocks and to constrain their source regions, with reference to primordial mantle or N-MORB compositions. For this purpose all the samples from Plio-Pleistocene volcanic rocks from the Chagai arc are plotted in primordial mantle normalized spider diagram (Fig. 9) with an average trace element spider plot of N-MORB for comparison (both normalizing and average values are after Sun and McDonough (1989).

The spider patterns in this diagram exhibit enrichment of whole range of incompatible trace elements except Ti and Y relative to N-MORB, which are consistent with an enriched sub-arc mantle peridotite source. The patterns exhibit marked negative slope from LILE to HFSE marking high LILE/HFSE ratios, which are evident for the incorporation of higher amount of LILE enriched subduction-related fluids in the sub-arc magma source. The patterns also show negative Nb anomalies and positive spikes generally on Ba and Sr, similar to those of island arcs volcanics.

Chondrite Normalized REE Diagrams: Chondrite normalized REE diagrams are generally prepared to determine the behavior of REE in the rocks and to constrain their source compositions, with reference to normalized chondritic values. The rocks show (Fig. 10) progressively enriched LREE patterns as compared to average N-MORB REE pattern (after Sun and McDonough, 1989). The MREE (Sm, Eu and Gd) and HREE (Er & Yb) show variable depletion as compared to average N-MORB. Most of the samples have variably developed positive Eu anomalies.

5. Petrogenesis

5.1. Nature of Parent Magma

The orogenic andesites for which parent magma was directly derived from the sub-arc mantle source must have higher MgO wt. % (> 6), higher Mg # (> 67), Low (< 1.1) FeOt/MgO ratios and higher concentration of Ni (> 100 ppm) and Cr (> 500 ppm) content (Gill, 1981). The Plio-Pleistocene andesites from the Chagai arc have low concentrations of MgO (2.89-4.8 wt. %), higher values of FeOt/MgO ratios (1.28-2) and low values for Mg # (50-56). However, one andesite from KSV volcanics has 5.90 wt. % MgO, Mg # = 64, and FeOt/MgO ratio = 1.01. All analyses also have low contents of Co (16-50), Ni (7-68) and have enhanced LILE/HFSE and LREE/REE ratios. Therefore, it is concluded that the parent magma of these rocks has not been directly derived from an upper mantle peridotite source, but underwent olivine fractionation en route to eruption, most probably in an upper level magma chamber.

The higher Zr/Y (5.07-9.08), Zr/Nb (17.75-28.75), Ti/V (24.22-33.91), La/Yb (9.07-11.87), Ta/Yb (0.11-1.18) and Th/Yb (1.69-2.25) ratios in these volcanics (Tables 1) are found close to the reported (Gill, 1981; Shervais, 1982; Wilson, 1989) values of these ratios in the volcanic rocks of continental margin type arcs rather than in similar rocks of oceanic island arcs.

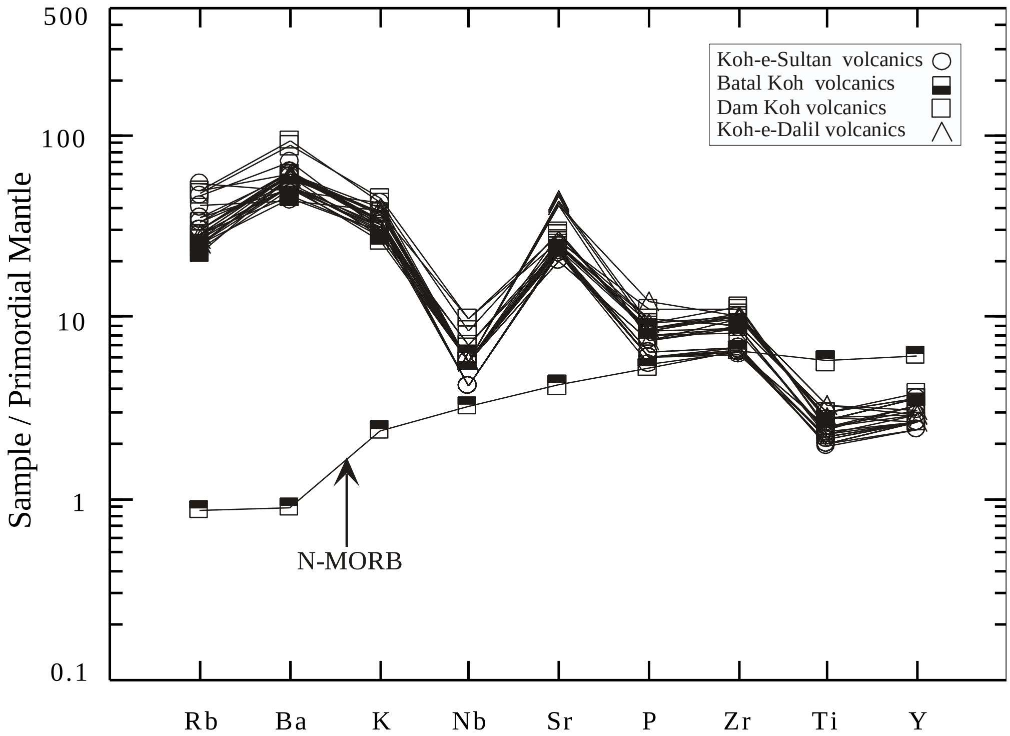

Fig. 9. Primordial mantle normalized spider diagram for the Plio-Pleistocene volcanic rocks from the Chagai arc. The half filled square pattern is for average N-MORB. Average N-MORB and normalization values are after Sun and McDounough (1989).

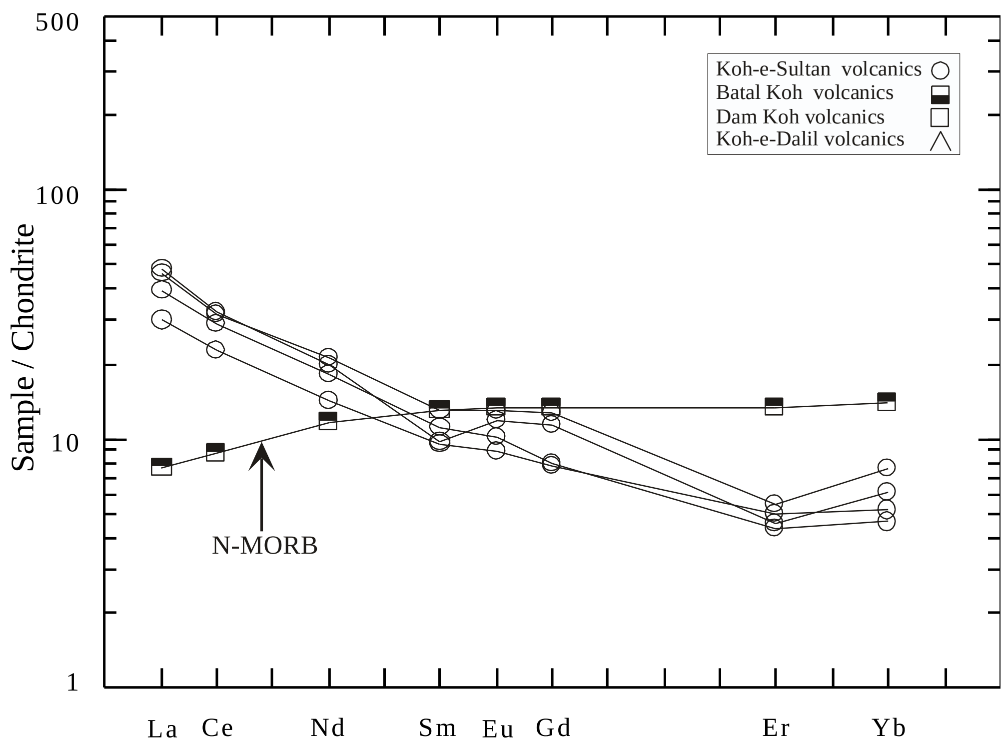

Fig. 10. Chondrite normalized REE diagram for the Plio-Pleistocene volcanic rocks from the Chagai arc. The half filled square pattern is for average N-MORB. Average N-MORB values are after Sun and McDounough (1989), whereas normalization values are after Nakamura (1974).

5.2. Tectonic Setting

A number of plots and tectonomagmatic discrimination diagrams based on major, minor or trace elements are designed to study the parent magma and tectonic setting of the volcanic rocks. Diagrams based on major elements or large ion lithophile (LIL) elements must be used with caution, as these elements are more mobile during post-magmatic alteration or metamorphic processes as compared to high field elements (Pearce and Can, 1973; Floyed and Winchister, 1975; Weaver and Tarney, 1981).

The FeO/MgO ratios generally show higher values in tholeiitic assemblages for a given SiO_2 content (Miyashiro; 1974; Gill, 1981). The SiO_2 versus FeO/MgO plots (Miyashiro, 1974) for all the samples reveal that most of the Plio-Pleistocene volcanic rocks are calc-alkaline in nature (Fig. 11A). To ascertain whether the studied rocks were erupted in an oceanic island arc environment or in a continental margin-type arc settings, the sample are plotted in Zr versus Zr/Y plot (after Pearce, 1983). In this diagram (Fig. 11B), all the sample plot in continental margin-type arc domain. The discrimination diagram based on trace element ratios is considered more authentic. The Th/Yb versus Ta/Yb plot of Pearce, (1983) is widely used, not only for the determination of tectonic environment but also for the estimation of nature of source (enriched or depleted), crustal contamination, within-plate enrichment and fractionation, etc. A plot of the KSV volcanics in this diagram (Fig. 11C) confirms their continental margin-type arc affinities. The plot of the analyses in this diagram further suggests that the parent magma of these volcanics was generated by an enriched mantle source.

The spider patterns (Fig. 9), which exhibit positive spikes generally on K and Sr and marked negative anomalies on Nb, further confirm the island arc signatures of the rocks (Pearce, 1982; Wilson 1989; Saunders et al., 1991). The marked negative Nb anomalies are explained by retention of this element in the residual mantle peridotite source during its partial melting. The positive spikes or enrichment of certain LIL elements are generally considered to have formed by incorporation of these elements in the source from the subducting slab (Pearce, 1982; Wilson, 1989).

5.3. Nature of the Source of Parent Magma

The Zr versus Zr/Y diagram (Fig. 11D) provides useful information about the nature of source, degree of partial melting and fractionation, etc. Plots of the analyses in this diagram indicate that these rocks are fractionated from 15 % partially melted enriched mantle source. The plots also indicate that the KSV volcanics were fractionated from a least enriched source as compared to KDV, DKV and BKV volcanics, which were developed in progressively increasing enriched sources. This diagram further suggests that KSV volcanics are least fractionated as compared to other volcanics, which show an overlapping increase in fractionation.

6. Comparison with other arcs

In Table 2, average trace element chemistry of the Plio-Pleistocene calc-alkaline volcanic rocks of the Chagai arc is compared with average calc-alkaline rocks of continental margin type arcs, including Andes, Zagros, Sunda, and Japan arcs, and oceanic island arcs including Mariana South West Pacific arcs, Fiji and New Britain arcs. This comparison shows close affinities of the Plio-Pleistocene volcanic rocks of the Chagai arc with continental margin type arcs rather than those of the oceanic arcs. The average andesite from the Chagai arc shows closer similarity in LILE, HFSE and REE and their ratios with its counterpart in Zagros arc, and less with Japan and Sunda arcs It greatly differs in these elements with its counterpart in Andes arc (Table 2).

Table 2. A comparison of average trace element chemistry of Plio-Pleistocene calc-alkaline andesites from the Chagai arc with some arc related andesites of the world

Trace Elements & Ratio	Chagai Arc	Continental Margin Arcs				Oceanic Island Arcs		
		Japan 1	Sunda 2	Zagros 3	Andes 4	Mariana 5	New Britain 6	Fiji Arc 7
Ti	3320	4080	4732	—	5691	4800	58.90	4140
Rb	19.54	36	39	23	75	12.67	11	20
Sr	563	294	466	619	648	378	384	490
Ba	384.73	318	437	271	886	348	185	522
V	121.69	172	153.8	—	125	186	340	172
Cr	79.77	67.5	19	104	48	23.67	34	39
Co	21.88	21	—	18	19	31.33	—	16
Ni	17.23	35.5	10.8	—	39	10.33	23	9
Zr	97.12	123	84.80	—	195	70.6	34	114
Y	13.92	19	21.6	—	12	24	12	18
Nb	4.12	3	2.8	—	—	1.1	0.9	2
Hf	1.58	3.8	—	—	5.46	—	—	2.3
Ta	0.51	0.14	—	—	—	—	—	—
Th	2.06	3.4	—	—	—	—	—	1.8
U	1.58	1.4	—	—	—	—	—	0.75
Sc	19.12		18.6	13	—	—	—	39
Cu	—	45.3	—	—	40	103	—	36
La	12.73	9.7	12.85	15	38	30.6	3	11
Ce	24.17	23	27.96	34.2	66.8	25.3	10	27
Nd	11.30	12	16.07	—	—	23.33	—	—
Sm	2.28	3.3	3.45	2.75	—	20.37	—	—
Eu	0.82	0.90	1.12	1.01	—	17.1	—	—
Gd	2.63		—	—	—	18.03	—	—
Er	1.11		—	—	—	12.9	—	—
Yb	1.28	2.2	1.50	1.48	1.94	11.2	—	—
Ti/V	28.50	23.72	30.77	—	45.60	25.81	10.06	24.07
Zr/Y	6.98	6.47	3.93	—	15.98	2.94	2.83	6.33
Ti/Zr	34.85	33.17	55.80	—	29.23	67.99	100.59	36.32
Zr/Nb	23.93	4140	30.29	—	—	64.18	37.78	57
La/Yb	10.16	4.40	8.57	10.14	19.49	2.73	—	—
Ce/Yb	19.42	10.45	18.64	23.11	34.43	2.26	—	—

The values in column 1 are after Govindaraju, (1989), 2 after Wheller et al. (1987), 3 after Dupuy and Dostal (1978), 4 after
Ewart (1982), 5 after Woodhead (1988), 6 and 7 after Gill (1981). All the data in ppm.

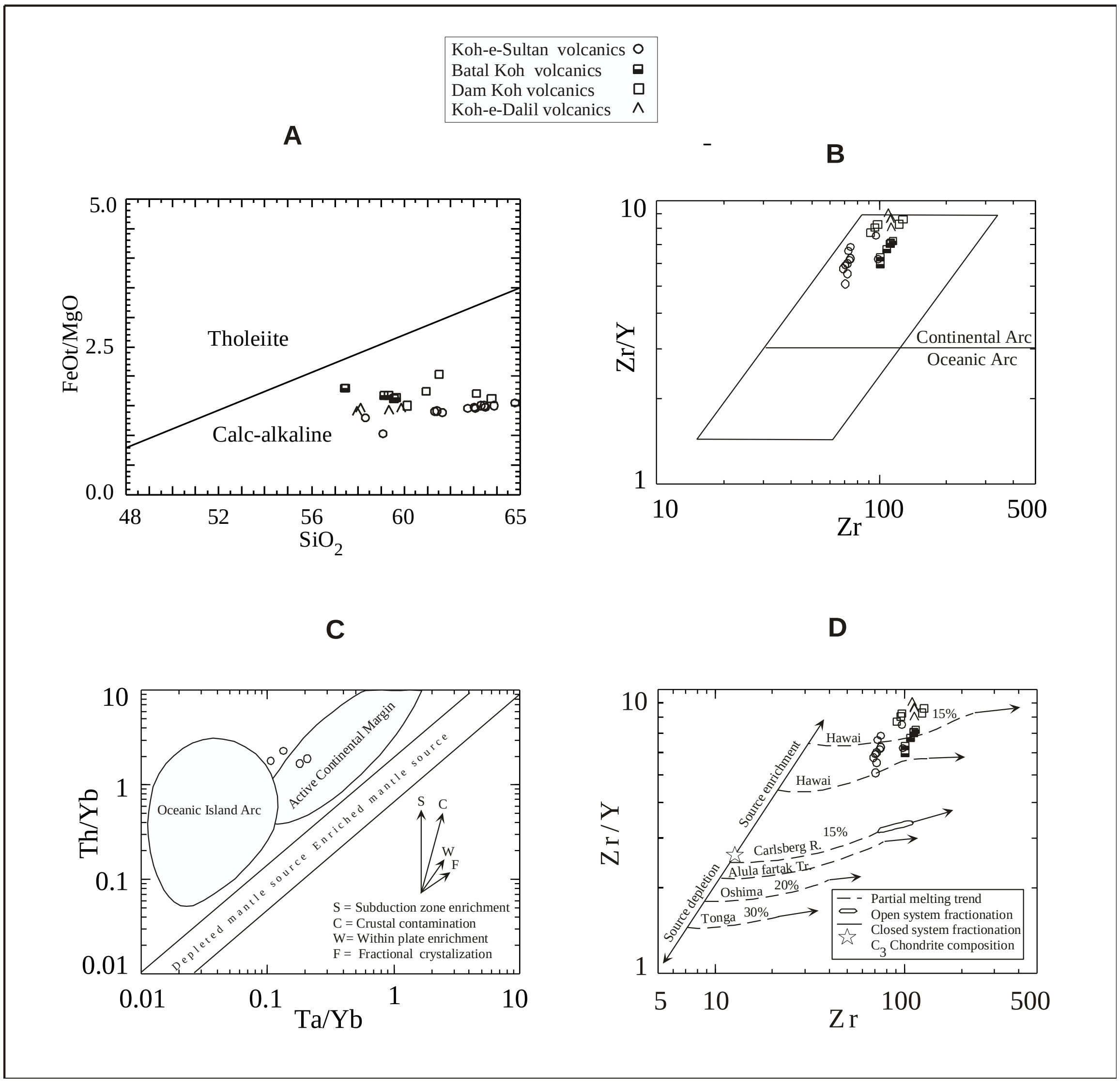

Fig. 11 A to D. Various tectonomagmatic discrimination diagrams for the Pli-Pleistocene volcanic rocks from the Chagai arc (see the text for details).

7. Discussion

The petrological and geochemical data presented in this paper strongly suggest that the Plio-Pleistocene volcanic rocks represent a calc-alkaline association of continental margin-type arc and the parent magma of these rocks was fractionated from an enriched sub-arc mantle source. The Plio-Pleistocene Koh-e-Sultan volcanism and the synchronous volcanism in Iran are considered to be related with convergence of Arabian oceanic plate below the southern margin of Afghan and Iran blocks, respectively (Jacob and Quittmeyer, 1979; Arthurton et al., 1979; Dykstra and Birnie, 1979: Dupuy and Dostal, 1978). Dykstra and Birnie (1979) have proposed a segmented Quaternary (now Plio-Pleistocene) subduction zone based on termination and offset in the belt of these volcanics and distribution of earthquake epicenters in this region. They proposed four NS trending segments, designated as A, B, C and D in Iranian and Pakistani Balochistan (Fig. 12), with a common hinge line near the Makran coast. The two outer segments A and D have shallow dips (10°- 20°) and are devoid of any volcanic activity, whereas the inner two segments, B (38°-50°) and C (19°-20°), have steeper dips and associated volcanism. Partial melting in subducted oceanic crust usually takes place at 110-173 km depth in the Beniof zone and the nature of parent magma is controlled by the dip angle of the subducted plate (Tatsumi and Eggens, 1995). Therefore, the NW-SE trend of the Plio-Pleistocne volcanic belt is attributed to the occurrence of volcanism in the B segment more southward, closer to the hinge line due to its steeper depth as compared to the C segment.

8. Conclusion

The petrogenetic studies of Plio-Pleistocene volcanic rocks suggest that they are calc-alkaline in nature and formed in a continental margin-type arc environment. Higher concentration of most HFSE, ΣREE and greatly enhanced Zr/Y, Ti/V, Ta/Yb, Th/Yb, La/Yb and Th/Yb ratio relative to N-MORB indicate that the parent magma of these rocks was derived from an enriched sub-arc peridotite mantle source. The Plio-Pleistocene andesites have low MgO wt. %, Mg # (50-56), and and contents of Co, Ni, but enhanced LILE/HFSE and LREE/HREE ratios, which suggests that the source magma of these rocks was not derived directly from an upper mantle peridotite source, but instead had undergone olivine fractionation en route to eruption. The Zr versus Zr/Y studies suggest that the parent magma was generated by about 15 % partial melting of an enriched sub-arc mantle source that fractionated in an upper level magma chamber. It is also suggested that the Koh-e-Sultan volcanics were generated by relatively higher degree of partial melting of a least enriched sub-arc mantle source and exhibit minimum fractionation as compared to the volcanics in Batal Koh, Dam Koh and Koh-e-Koh Dalil volcanoes. The latter shows the lowest degree of partial melting of a most enriched sub-arc mantle source that underwent more fractionation than the rest. A comparison of average calc-alkaline andesite from Plio-Pleistocene volcanics of the Chagai arc with its counterparts in some famous continental margin and oceanic island arcs of the world show relatively more resemblance in LILE, HFSE and REE with Zagros, less with Japan and Sunda arcs, and least with its counterpart in the Andes arc.

Acknowledgements

We are highly indebted to Dr. Imran Ahmad Khan, Director General, Geological Survey of Pakistan (GSP), Mr. S. Hasan Gauhar, ex-Director General, GSP, and Mr. Tahir Karim (Director) of the same Department for their support during field and laboratory research.

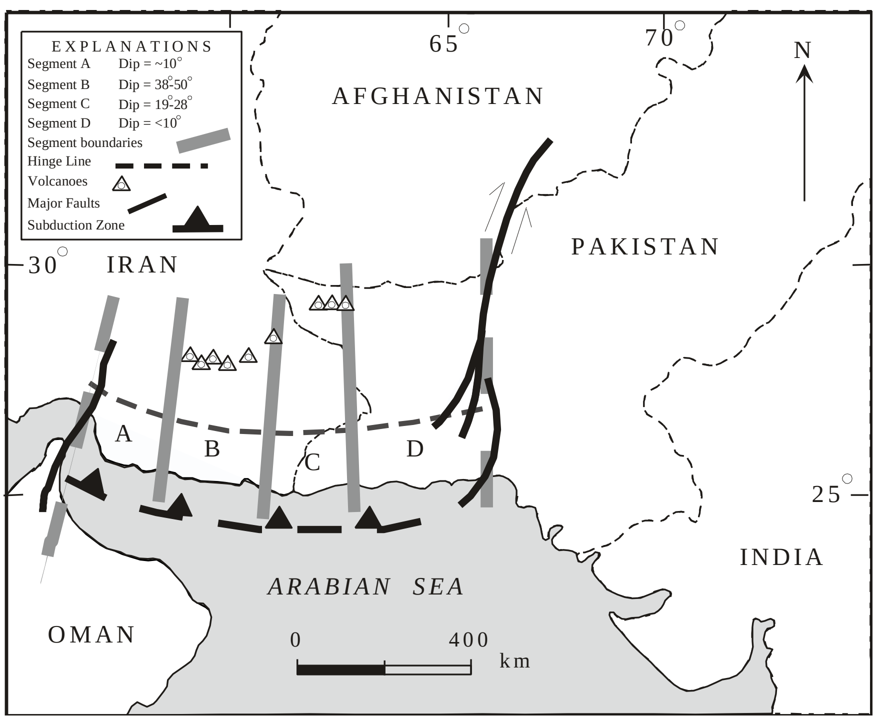

Fig. 12. Map showing proposed segmented subduction zone for Plio-Pleistocene (former Quaternary) volcanics in parts of Iranian and Pakistani Balochistan (after Dykstra and Birnie, 1979).

References

Arthurton, R.S., Alam, G.S., Ahmed, S.A., Iqbal, S., 1979. Geological history of Alam Reg - Mashki Chah area, Chagai District, Balochistan. In Farah, A., DeJong, K.A., (Eds.), Geodynamics of Pakistan. Geological Survey of Pakistan, 325-331.

Arthurton, R.S., Farah, A., Ahmed, W., 1982. The Late Cretaceous-Cenozoic history of western Balochistan, Pakistan - the northern margin of the Makran subduction complex. In Leggett, J. K., (Ed.), Trench Fore-Arc Geology, Geological Society of London Special Publication, 10, 343-385.

Bakr, M.A., Jackson, R. O., 1964. Geological Map of Pakistan. Geological Survey of Pakistan, Quetta.

Britzman, L., 1979. Fission track ages of intrusives of Chagai District, Balochistan,

Pakistan: Unpublished M.A. thesis, Darmouth College, Honover, N. H., U.S.A.

Dupuy, C., Dostal, J., 1978. Geochemistry of calc-alkaline volcanic rocks from southeastern Iran (Kouh-e-Shahsawaran). Journal of Volcanology and Geothermal Research., 4, 363-373

Dykstra, J. D., 1978. A geological study of Chagai Hills Balochistan, Pakistan using LANDSAT digital data. Unpublished Ph.D. Thesis, Dartmouth College, Hanover, N. H., U.S.A.

Dykstra, J.D., Birnie, W., 1979. Segmentation of the Quaternary subduction zone under the Balochistan region of Pakistan and Iran, In Farah, A., DeJong, K.A. (Eds.), Geodynamics of Pakistan. Geological Survey of Pakistan, 319-323.

Ewart, A., 1982. The mineralogy and petrology of Tertiary-Recent orogenic volcanic rocks with special reference to andesitic-basaltic compositional range, In Throp, R.S., (Ed.), Andesites: Orogenic Andesites and Related Rocks. John Wiley and Sons, New York, 26-87.

Farah, A., Abbas G., DeJong. K.A., Lawrence, R.D., 1984. Evolution of the Lithosphere in Pakistan. Tectonophysics, 105, 207-227.

Farah, A., Lawrence, R.D., DeJong. K.A., 1984. An overview of the tectonics of Pakistan, In Haq, B.U., Milliman, J.D., (Eds.), Marine geology and oceanography of Arabian Sea and coastal Pakistan. Van Nostrand Reinhold Company, New York, 161-176.

Floyd, P.A., Winchester, J.A., 1975. Magma types and tectonic setting discrimination using immobile elements. Earth and Planetary Science Letters, 27, 211-218.

Gill, J.B., 1981. Orogenic Andesites and Plate Tectonics. Springer, Berlin, 189.

Govindaraju, K., 1989. Geostandards Newsletter, Special Issue, Working Group on Analytical standards of minerals, ores and rocks. France, 13, 114.

Harker, A., 1909. The natural history of igneous rocks. Macmillan, New York

Hole, M.J., Saunder, A.D., Marriner, G.F., Tarney, J., 1984. Subduction of pelagic sediments; implication for the origin of Ce-anomalous basalts from Mariana Islands. Journal of Geological Society of London, 141, 453-472.

Imai, N., 1990. Multielement analysis of rock with the use of geological certified reference materials by inductively coupled plasma mass spectrometry. Analytical Science, 6, 389-385.

Jacob, K.H., Quittmeyer, R.L., 1979. The Makran region of Pakistan and Iran, In Farah, A., DeJong, K.A. (eds.), Geodynamics of Pakistan. Geological Survey of Pakistan, 303-317.

Jones, A.G., 1960. Reconnaissance Geology of Part of West Pakistan: A Colombo Plan Cooperative Project, Govt. of Canada, Toronto, (Hunting Survey Corporation report) 550.

Kazmi, A.H., Jan, M.Q., 1997. Geology and tectonics of Pakistan. Graphic Publishers, Karachi.

Le Bas, M.J., Le Maitre, R.W., Streckeisen, A., Zanettin, B., 1986. A chemical classification of volcanic rocks based on the total alkali silica diagram. Journal of Petrology, 27, 745-750.

Miyashiro, A., 1974. Volcanic rock series in island arcs and active continental margins. American Journal of Science, 274, 321-355.

Nakamura, N., 1974. Determination of REE, Ba, Fe, Mg, Na and K in carbonaceous and ordinary chondrites. Geochimica et Cosmochimca Acta, 38, 757-775.

Ogg, J,G., Ogg, G., Gradstein, F.M., 2008. The Concise Geological Time Scale, International Commission on Stratigraphy (www.stratigraphy.org)

Pearce, J.A., 1982. Trace elements characteristics of lavas from destructive plate boundaries. In Throp, R.S. (Ed.), Andesites: Orogenic andesites and related rocks. John Wiley and Sons, New York, 525-548.

Pearce, J.A., 1983. The role of subcontinental lithosphere in the magma genesis at destructive plate margin, In Hawkes-worth, C.J., Norry, M.J., (Eds.), Continental basalts and mantle xenoliths. Natwich Shiva, 230-249

Saunders, A.D., Tarney, J., 1991. Back-arc basins. In: Floyd. P.A. (Ed.), Oceanic Basalts, Blackie, London, 219-263.

Shareq, A., Chmyriov, V.M., Stazhilo-Alekseev, K.F., Dronov, V.I., Gannon, P.J., Lubemov, B.K., Kafarskiy, A.K.H., Malyarove, E.P., 1977. Mineral Resources of Afghanistan. (2nd ed.), Afghan Geological and Mines Survey, Afghanistan.

Shervais, J.W. (1982). Ti versus V plots and the petogenesis of modern and ophiolitic lavas. Earth and Planetary Science Letters, 59, 101-108.

Siddiqui, R.H., 1996. Magmatic evolution of Chagai-Raskoh arc terrane and its implication for porphyry copper mineralization. Geologica, 2, 87-119.

Siddiqui, R.H., Khan, M.A., Naseem, M., 2002. Geology and petrogenesis of Pliocene to Pleistocene volcanic rocks from the Chagai arc Balochistan Pakistan. Published by the International Division, Geological Survey of India in the Vol. of Abstracts, Fourth South Asia Geological Congress (GEOSAS-IV).

Siddiqui, R.H., 2004. Crustal evolution of the Chagai-Raskoh arc terrane, Balochistan, Pakistan. Unpublished Ph.D. Thesis, Centre of Excellence in Geology, University of Peshawar, Pakistan.

Siddiqui, R.H., Khan, M.A., Jan M.Q., 2005. Petrogenesis of Eocene Lava flows from the Chagai Arc, Balochistan, Pakistan and its tectonic implications. Geol. Bulletin of University of Peshawar, 38, 163-187.

Sillitoe, R.H., 1978. Metallogenic evolution of a collision mountain belt in Pakistan: a preliminary analysis. Journal of Geological Society of London, 125, 377-387.

Sun, S.S., McDonough, W.F., 1989. Chemical and isotopic systematics of ocean basalt, implication for mantle composition and processes. In Saunders, A.D., Torny, M.J., (Eds.), Magmatism in the ocean basins. Journal of Geological Society of London (Special Publication), 42, 313-345.

Tatsumi, Y., Eggins, S., 1995. Subduction Zone Magmatism. Blackwell Science, Oxford, England, 211.

Taylor, S.R., McLennan, S.M., 1985. The continental crust: its composition and evolution. Blackwell, Oxford.

Vredenburg, E.W., 1901. A geological sketch of the Balochistan desert and part of Eastern Persia. Geological Survey of India, Memoirs, 302.

Weaver, B.L., Tarney J., Windley, B., 1981. Geochemistry and petrogenesis of the Fiskenaesset anorthosite complex southern West Greenland: nature of the parent magma. Geochimica et Cosmochimica Acta, 45, 711-725.

Wheller, G.E. Varne, R., Foden, J.D., Abbott, M.J., 1987. Geochemistry of Quaternary volcanics in the Sunda-Bunda arc Indonesia, and three component genesis of island arcs basaltic magma. Journal of Volcanology and Geothermal Research, 32, 137-160.

Wilson, M., 1989. Igneous Petrogenesis. Unwin and Hyman, London, 466.

Winchester, J.A., Floyd, P.A., 1977. Geochemical discrimination of different magma series and their differentiation products using immobile elements: Chemical Geology, 20, 325-343.

Woodhead, J.D., 1988. The origin of geochemical variations in Mariana lavas. A general model for petrogenesis in intra oceanic island arc. Journal of Petrology, 29, 805-830.